ELSEVIER

Journal of Nuclear Materials 278 (2000) 273–276

journal of nuclear materials

www.elsevier.nl/locate/jnucmat

Phase diagram and lattice instability in tungsten–rhenium alloys

M. Ekman, K. Persson, G. Grimvall *

Theoretical physics, Royal Institute of Technology, SE-100 44 Stockholm, Sweden

Received 21 May 1999; accepted 17 September 1999

Abstract

Tungsten has been suggested as a material in applications where it is irradiated by neutrons and undergoes transmutation to rhenium. Pure W has the bcc lattice structure. According to the equilibrium phase diagram about 30 at.% Re can go into a bcc W–Re solid solution. However, ab initio electronic structure calculations show that the bcc lattice becomes dynamically unstable at high Re concentrations. Through a detailed calculation of the phonon spectrum, we find that bcc $W_{1-c}Re_c$ does not become dynamically unstable until $c \gtrsim 0.7$, i.e., well above the equilibrium solubility limit of Re in bcc W. Concentration fluctuations of Re in irradiated W will therefore not lead to any significant number of regions where the bcc lattice collapses due to a dynamical instability.

PACS: 41.Qb; 81.30.-t; 81.30.Bx; 63.20.-e

1. Introduction

Tungsten is of interest as a shielding material in fusion reactors and other systems with nuclear reactions [1–3]. Under neutron irradiation, tungsten may transmute to rhenium. In certain applications and after long service as many as 25% of the W atoms have been transmuted [1]. This is still within the region of a bcc solid solution of Re in W (Fig. 1(a)). However, ab initio electronic structure calculations performed by us [4] show that the bcc lattice structure of pure Re is dynamically unstable against several different lattice distortions, leading to fcc, hcp, dhcp and ω-phase lattice structures. For instance, the elastic shear constant $C' = (c_{11} - c_{12})/2$ is negative in bcc Re. Hence, there is a critical concentration $c = c^*$ of Re atoms at which a bcc W–Re solid solution would become dynamically unstable. It is the purpose of this paper to discuss the consequences of such an instability when tungsten is used as a material subject to heavy neutron irradiation.

The paper is organized as follows. In Section 2 we give the Helmholtz energy of bcc W–Re. The implication for the W–Re phase diagram is dealt with in Section 3, and Section 4 considers the possibility of local concentrations $c > c^*$ in an irradiated material for which the overall Re concentration is less than c^*. The paper ends with a discussion in Section 5 and conclusions in Section 6.

2. The Helmholtz energy of bcc W–Re alloys

The details of our ab initio electronic structure calculations of lattice energies and phonon frequencies are reported elsewhere [4]. Here we summarize those results that are necessary for our discussion of the phase diagram. The Helmholtz energy $F(c) = U(c) - TS(c)$ of a $W_{1-c}Re_c$ alloy with a certain lattice structure has three important contributions:

$$F_{\mathrm{tot}}(c) = F_{\mathrm{conf}}(c) + F_{\mathrm{el}}(c) + F_{\mathrm{ph}}(c), \tag{1}$$

where $F_{\mathrm{conf}}(c)$ is the Helmholtz energy of a static lattice in which the atoms take an equilibrium configuration,

* Corresponding author. Tel.: +46-8 790 7174; fax: +46-8 104 879.

E-mail address: grimvall@theophys.kth.se (G. Grimvall).

0022-3115/00/$ - see front matter
PII: S0022-3115(99)00241-X

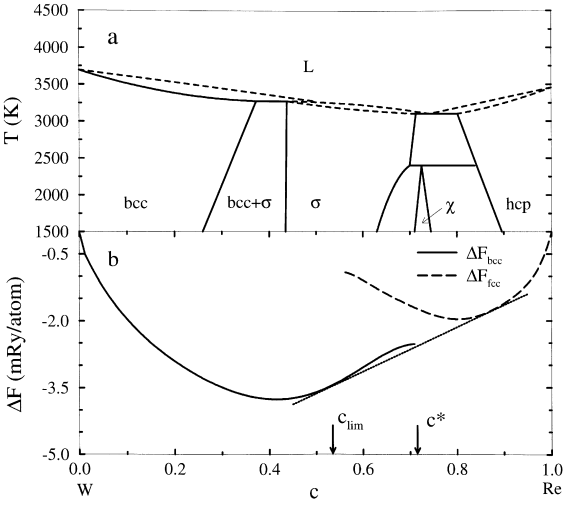

Fig. 1. The upper panel (a) shows the experimentally determined phase diagram. The lower panel (b) shows the Helmholtz energy difference ΔF at $T = 1500$ K, as derived from our ab initio electron structure calculations and used here in a conventional 'tangent' construction for phase diagrams.

and the electrons are in their ground state. F_{conf} for an element (here W or Re) is easily calculated and can be identified with the cohesive energy of a static lattice at 0 K. When $0 < c < 1$ we use a standard cluster-expansion technique [5,6] to obtain the energy U of various atomic configurations of W and Re atoms. The entropy is obtained by using the cluster-variation method [7]. At the high temperatures of interest for the equilibrium phase diagram (typically $T > 1000$ K) the entropy is found to be well described by $S_{\text{random}} = -k_{\text{B}}[c \ln c + (1-c)\ln(1-c)]$ per atom, showing that there is negligible short range order. Therefore, $F_{\text{conf}}(c) \approx U_{\text{random}}(c) - TS_{\text{random}}(c)$, where $U_{\text{random}}(c)$ refers to a random bcc W–Re substitutional solid solution.

The contribution from electronic excitations, $F_{\text{el}}(c)$, is in our case well represented by the Sommerfeld-type expression

$$F_{\text{el}}(c) = -\frac{\pi^2}{6} N(E_{\text{F}}; c)(k_{\text{B}}T)^2, \tag{2}$$

where $N(E_{\text{F}})$ is the electron density of states at the Fermi level E_{F}. $N(E_{\text{F}}; c)$ is obtained by a linear interpolation in the concentration c between $N(E_{\text{F}})$ for pure bcc W and bcc Re, respectively. This approximation, of rigid-electron-band type, is reasonable since W and Re are neighbours in the Periodic Table.

The most difficult part to account for, and of central interest here, is the contribution F_{ph} from lattice vibrations. It requires the calculation of individual phonon frequencies $\omega(\boldsymbol{q}, s)$ of wave vector $\boldsymbol{q}$ and mode s (longitudinal and transverse) for enough $\boldsymbol{q}$-points such that a representative phonon density of states can be formed. This is a straight-forward task for elemental bcc W and bcc Re, but not feasible for a random $W_{1-c}Re_c$ solid solution. Tungsten in the observed bcc structure of course has all $\omega^2(\boldsymbol{q}, s) > 0$. However, as mentioned in the introduction, there are large regions of $\boldsymbol{q}$-vectors in the first Brillouin zone for which the phonon modes in bcc Re have $\omega^2 < 0$, implying a dynamically unstable lattice.

The following interpolation procedure is now used to estimate $\omega^2(\boldsymbol{q}, s; c)$ for bcc $W_{1-c}Re_c$. For the disordered system the virtual crystal approximation [8] (VCA) is applied. The phonon dispersion curves are calculated for a set of different concentrations $(c = 0.25; 0.50; 0.75)$ and fitted to a standard Born–von Kármán force constant model. The force constants are then interpolated by a cubic spline in the concentration c, from W (i.e., $c = 0$) to Re $(c = 1)$. This is a reasonable procedure because the force constants reflect changes in the electronic structure, and W and Re are neighbours in the Periodic Table.

On the basis of these force constants, we solve for $\omega^2(\boldsymbol{q}, s; c)$ and find the highest concentration $c = c^*$ for which all $\omega^2(\boldsymbol{q}, s; c) > 0$, i.e., the critical composition for dynamical lattice instabilities. In bcc W–Re this procedure yields $c^* = 0.71$. When $c < c^*$ our set of force constants easily gives the phonon frequencies for any phonon state $(\boldsymbol{q}, s)$ and concentration c. We then calculate the Helmholtz energy. Its essential features can be seen from the leading high-temperature term (per atom; $T > \theta_{\text{D}}$ where θ_{D} is a characteristic Debye temperature ~320 K for W)

$$F_{\text{ph}} \approx -3k_{\text{B}}T \ln\left[\frac{k_{\text{B}}T}{\hbar\omega_{\log}}\right]. \tag{3}$$

Here $\omega_{\log}(c)$ is the logarithmically averaged phonon frequency.

3. Phase diagram considerations

To determine the true phase diagram one must consider the Helmholtz energy of all competing phases. Because our main concern is the dynamical instability of the bcc phase, we consider the competition between a bcc W–Re solid solution as described above and a reference phase which we choose to be fcc W–Re. (The observed structure of pure Re is hexagonal close-packed, but fcc Re is dynamically stable and choosing the fcc phase instead will not affect the conclusions of this paper.) Thus, using the formalism in Section 2, we study

$$\Delta F_{\text{bcc}} = F_{\text{tot}}(\text{bcc } W_{1-c}Re_c) - (1-c)F_{\text{tot}}(\text{bcc W}) - cF_{\text{tot}}(\text{fcc Re}), \tag{4}$$

$$\Delta F_{\rm fcc} = F_{\rm tot}(\text{fcc } W_{1-c}Re_c) - (1-c)F_{\rm tot}(\text{bcc W}) - cF_{\rm tot}(\text{fcc Re}). \quad (5)$$

As an illustrating example, the contributions to $\Delta F_{\rm bcc}$ for $W_{29}Re_{71}$ are (in mRy/atom) $\Delta F_{\rm config} = +5.36$, $\Delta F_{\rm ph} = -7.47$ and $\Delta F_{\rm el} = -0.43$; cf. also Fig. 6 in Ref. [4]. To illustrate the possible effect of the bcc lattice instability on the equilibrium W–Re phase diagram, we show ΔF in Fig. 1(b) for $T = 1500$ K. Fig. 1(a) gives the phase diagram as determined in the experiments [9,10]. The function $\Delta F_{\rm bcc}$ ends at $c = c^* = 0.71$, where in our model the bcc lattice becomes dynamically unstable. Beyond this concentration, the vibrational entropy of the hypothetical bcc structure has no meaning and hence the Helmholtz energy is undefined. (Quantities like S and F are defined for phases in stable or metastable thermodynamic equilibrium, but not for a *dynamically* unstable phase.)

As expected, in Fig. 1(b) the critical concentration c^* falls beyond the observed range of the bcc W–Re solid solution. The question now arises if there are any precursors to be seen in the phase diagram when $c < c^*$. The dashed line is drawn in analogy to the standard technique of a 'common tangent' construction in curves of $F_{\rm tot}$ versus c that is used to find the limiting concentrations of the phase-field boundaries. As drawn in the figure, it defines a concentration $c_{\rm lim}$ that has the following interpretation. In a thermodynamic competition between bcc and fcc W–Re, the phase diagram shows a bcc solid solution up to $c = c_{\rm lim}$ and is followed beyond that concentration by a two-phase field with bcc and fcc W–Re. In the actual W–Re system, the two-phase field contains bcc W–Re and the σ-phase; cf. Fig. 1(a) and Ref. [11]. The corresponding concentration $c_{\rm lim}$ would result if we had known $F_{\rm tot}$ of the σ-phase and made the tangent construction. We conclude that the dynamical instability in the bcc phase at $c \approx 0.71$ falls well beyond the observed solubility limit of Re in bcc W, and therefore has no significant precursor effect on the bcc phase field in the equilibrium W–Re phase diagram. This is in agreement with analogous conclusions for W–Pt and other alloys [12,13]. However we note that undercooled liquid W–Re alloys with 50 at.% W may solidify in a metastable bcc structure [14].

4. Local fluctuation in the alloy composition

We assume that the transmutation of W to Re leads to a truly random substitutional bcc solid solution of a certain average composition c_0. Thus we disregard, e.g., the creation and influence of lattice defects, and annealing effects caused by the diffusion of atoms. Given the average composition c_0, there will be local fluctuations of a statistical nature. It is of interest to find the probability that in a small region the concentration c is so large that the bcc lattice becomes dynamically unstable there, in spite of the fact that c_0 is well within the range of a bcc phase in the phase diagram. Our calculation of the critical composition $c^* = 0.71$ referred to a macroscopically large system. We now consider a small region in the bcc W–Re lattice, approximately cubic in shape and containing N atoms ($N \gg 1$). Let c_0 be the probability that a lattice site is occupied by a Re atom. $P(N, c^*; c_0)$ is the probability that at least c^*N of the N sites are occupied by Re atoms, i.e., the local concentration in the considered region is $c \geqslant c^*$. $P(N, c^*; c_0)$ is obtained from binomial coefficients as

$$P(N, c^*; c_0) = \sum_{n=Nc^*}^{N} \binom{N}{n} c_0^n (1-c_0)^{N-n}. \quad (6)$$

We next want to calculate how many such regions, $R(c^*; c_0)$, of high local Re concentration there are in a certain macroscopic specimen. In its general formulation this is a very difficult statistical problem. For our purpose it suffices with an estimate of R (in fact, a lower bound) obtained as follows. Let the macroscopic volume be divided into s cubes, each containing N atomic sites. Then $R = sP(N, c^*; c_0)$. Fig. 2 shows the number, R, of overcritical regions per 1 cm^3, as a function of the size N of the small regions (cubes) and for four average Re concentrations c_0 in the specimen.

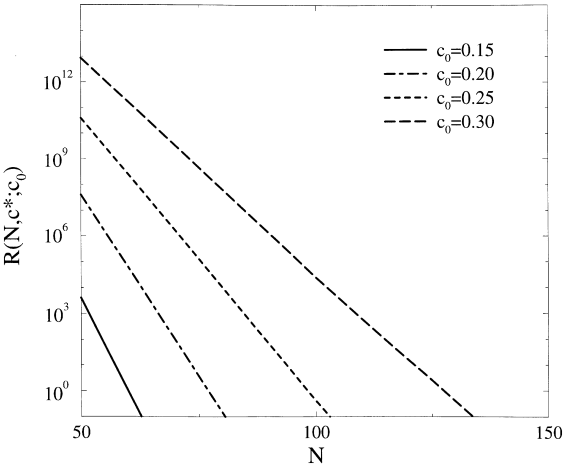

Fig. 2. $R(N,c^*;c_0)$ is the number of regions (cubes), per cm^3 of the W–Re specimen, in which the concentration of Re atoms is larger than c^*. $R(N,c^*;c_0)$ is plotted as a function of N, the number of atoms (lattice sites) in the considered small regions (cubes). Results are given for four overall Re concentrations c_0 in the specimen.

5. Discussion

Pure bcc Re is dynamically unstable for long-wavelength vibrational modes (sound waves) as well as for phonons of very short wavelength (Brillouin-zone-boundary states). In our model, the dynamical instability that is first encountered refers to a phonon with a wavelength equal to $0.87a$ where a is the bcc-W lattice parameter. Therefore, even a small region with $c > c^*$ may be associated with a local dynamical lattice instability. As an example, let us assume that a region containing a total of 100 atoms with $c > c^*$ suffices to develop an instability, i.e., consider $N = 100$. It is clear from Fig. 2 that the concentrations of such overcritical regions is negligibly small for all Re concentrations in the equilibrium bcc W–Re phase field.

We have ignored the subsequent transmutation of Re to Os [1,2]. In the Periodic Table Os follows after W and Re in the 5d transition-metal row. Both Re and Os have stable hcp lattice structures and a dynamically unstable bcc lattice [15,16]. In a rigid-band description of the electronic states, $W_{1-2c}Re_{2c}$ would be equivalent with $W_{1-c}Os_c$ for $c \leqslant 0.5$. This will lower the stability limit of the bcc W–Os lattice towards the bcc phase boundary at $c \approx 0.3$ in the equilibrium W–Re phase diagram, but it is still very unlikely that composition fluctuations due to neutron irradiation of bcc W will lead to a significant number of overcritical regions where the bcc lattice collapses.

Finally, we remark that our analysis ignores atomic diffusion as well as radiation damage. Since the transformation of W to Re takes place during a long time span, there may be time enough for diffusion to keep the local Re concentration close to its average value and thus very much below c^*. We also note that WRe and WRe_3 phases have been observed [17,18] in irradiated W at average Re concentrations below the solubility limit of Re in bcc W.

6. Conclusions

Ab initio calculations show that the bcc substitutional solid solution of $W_{1-c}Re_c$ is dynamically unstable beyond a critical concentration c^*. This may have important consequences when W is used as a material under heavy neutron irradiation, causing transmutation of W to Re. However, we find that the bcc lattice structure does not become dynamically unstable until $c \gtrsim 0.7$, i.e., well above the equilibrium solubility limit of Re in bcc W. Hence, in the bcc phase field of the equilibrium W–Re phase diagram (i.e., $c < 0.3$) one may ignore local statistical fluctuations in the Re concentration that would lead to small regions of dynamical lattice instability. Furthermore, the incipient bcc instability at $c \approx 0.7$ gives no significant precursor effects in the bcc phase field ($c < 0.3$).

Acknowledgements

This work was supported by the Swedish research foundation SSF. Most of the calculations were performed at the Swedish primary national source for high-performance computing and networking, Parallelldatorcentrum – PDC. Discussions with Professor Lars Holst on statistical problems are gratefully acknowledged.

References

[1] L.R. Greenwood, F.A. Garner, J. Nucl. Mater. 212–215 (1994) 635.
[2] C.B.A. Forty, G.J. Butterworth, J.-Ch. Sublet, J. Nucl. Mater. 212–215 (1994) 640.
[3] S.A. Fabritsiev, V.A. Gosudarenkova, V.A. Potapova, V.V. Rybin, L.S. Kosachev, V.P. Chakin, A.S. Pokrovsky, V.R. Barabash, J. Nucl. Mater. 191–194 (1992) 426.
[4] K. Persson, M. Ekman, G. Grimvall, Phys. Rev. B 60 (1999) 9999.
[5] J.M. Sanchez, F. Ducastelle, D. Gratias, Physica A 128 (1984) 333.
[6] J.W.D. Conolly, A.R. Williams, Phys. Rev. B 27 (1983) 5169.
[7] R. Kikuchi, Phys. Rev. 81 (1951) 988.
[8] L. Nordheim, Ann. Phys. (Leipzig) 9 (1931) 607.
[9] J.M. Dickinson, L.S. Richardson, Trans. Am. Soc. Metals 51 (1959) 758.
[10] B. Predel, in: O. Madelung (Ed.), Landolt–Börnstein New Series group IV, vol. 5, Springer, Berlin, 1998, p. 46.
[11] L. Kaufman, J.S. Watkin, J.H. Gittus, A.P. Miodownik, Calphad 1 (1977) 281.
[12] A. Fernández Guillermet, V. Ozoliņš, G. Grimvall, M. Körling, Phys. Rev. B 51 (1995) 10364.
[13] G. Grimvall, Ber. Bunsenges. Phys. Chem. 102 (1998) 1083.
[14] S. Tournier, M. Barth, D.M. Herlach, B. Vinet, Acta Mater. 45 (1997) 191.
[15] J.M. Wills, O. Eriksson, P. Söderlind, A.M. Boring, Phys. Rev. Lett. 68 (1992) 2802.
[16] K. Persson, M. Ekman, unpublished.
[17] R. Herschitz, D.N. Seidman, Acta Metall. 32 (1984) 1141.
[18] R. Herschitz, D.N. Seidman, Acta Metall. 32 (1984) 1155.